AD-A091 586 NAVAL RESEARCH LAB WASHINGTON DC F/G 9/5
ANALYSIS OF OSCILLATIONS IN THE GYROTRON TRAVELLING WAVE AMPLIF--ETC(U)
OCT 80 Y Y LAU, K R CHU, L BARNETT
UNCLASSIFIED NRL-MR-4303 NL

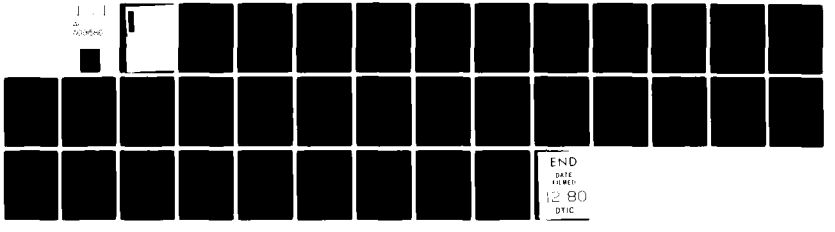

END
DATE FILMED
12 80
DTIC

(14) NRL--MR-4343

SECURITY CLASSIFICATION OF THIS PAGE (When Data Entered)

REPORT DOCUMENTATION PAGE

READ INSTRUCTIONS BEFORE COMPLETING FORM

1. REPORT NUMBER: NRL Memorandum Report 4303
2. GOVT ACCESSION NO.: AD-A091586
3. RECIPIENT'S CATALOG NUMBER:

4. TITLE (and Subtitle): (6) ANALYSIS OF OSCILLATIONS IN THE GYROTRON TRAVELLING WAVE AMPLIFIER
5. TYPE OF REPORT & PERIOD COVERED: Interim report on a continuing NRL problem
6. PERFORMING ORG. REPORT NUMBER:

7. AUTHOR(s): (10) Y. Y. Lau, K. R. Chu, L. Barnett, V. L. Granatstein
8. CONTRACT OR GRANT NUMBER(s): (9) Memorandum rept.

9. PERFORMING ORGANIZATION NAME AND ADDRESS: Naval Research Laboratory, Washington, DC 20375
10. PROGRAM ELEMENT, PROJECT, TASK AREA & WORK UNIT NUMBERS: NRL Problem 67-0863-0-0; Project No. XF62581007; Program Element-62762N

11. CONTROLLING OFFICE NAME AND ADDRESS: Naval Electronic Systems Command, Washington, DC 20360
12. REPORT DATE: (11) 29 October 1980
13. NUMBER OF PAGES: (12) 35

14. MONITORING AGENCY NAME & ADDRESS(if different from Controlling Office): (16) F62581; (17) XF62581007
15. SECURITY CLASS. (of this report): Unclassified
15a. DECLASSIFICATION/DOWNGRADING SCHEDULE:

16. DISTRIBUTION STATEMENT (of this Report)

Approved for public release; distribution unlimited.

17. DISTRIBUTION STATEMENT (of the abstract entered in Block 20, if different from Report)

18. SUPPLEMENTARY NOTES

*Science Applications, Inc., McLean, VA
†B-K Dynamics, Rockville, MD

19. KEY WORDS (Continue on reverse side if necessary and identify by block number)

gyrotron travelling wave amplifier
oscillations
grazing condition
instability

20. ABSTRACT (Continue on reverse side if necessary and identify by block number)

The operation of the gyrotron travelling wave amplifier is based on the convective cyclotron maser instability. It is found that this convective instability may become absolute (nonconvective) at a sufficiently high current level, resulting in oscillation instead of amplification. This threshold current for the transition depends sensitively on the applied magnetic field. The axial wavelength and the characteristic frequency of oscillation at the onset of absolute instability are given. It is found that momentum spread has virtually no effect on the threshold current. A small amount of resistive wall loss, however, raises the threshold current significantly. Oscillations due to partial
(Continued)

508

20. ABSTRACT (Continued)

reflection at the ends of the system are also examined. Preliminary experimental results on both types of oscillations are reported and are found to be in good agreement with the theory.

CONTENTS

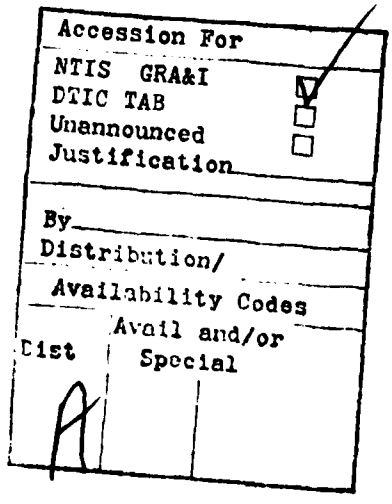

ANALYSIS OF OSCILLATIONS IN THE GYROTRON TRAVELLING WAVE AMPLIFIER

I. INTRODUCTION

Current experiments performed at NRL on the gyrotron travelling wave amplifier (gyro-TWA) have yielded record power levels at millimeter wavelengths.[1,2] However, the presence of unwanted oscillations has thus far prevented the operations of the amplifier in the optimum regime[2]. Significant improvement in performance is anticipated with the suppression of these unwanted oscillations. The main purpose of the present work is to investigate the possible causes of these oscillations and thereby to suggest ways for their suppression.

Oscillations are generally caused by either an external or an internal feedback process. The external feedback is provided by reflections at both ends of the interaction region. If the amplitude of the reflected signal reaches a certain level that the loop gain exceeds unity, the wave amplification processes become regenerative and oscillation consequently takes place. The internal feedback is a result of the dispersiveness of the unstable medium. Under certain conditions, the wave may grow locally without propagating axially out of the system. As a result, large amplitude waves can simply grow from noise level perturbations. Unlike those caused by end reflections, oscillations produced by internal feedback processes received comparatively little attention. Their considerations have special importance for the gyro-TWA in that the optimum operating regime of a gyro-TWA happens to border on the transition from the convective instability (amplification) to the absolute instability (oscillation).[3] Careful study of the internal feedback processes can therefore provide a guide for acheiving optimum operation of the gyro-TWA without the excitation of absolute instabilities.

Experimentally, there is convincing evidence that both types of oscillations are excited in the gyro-TWA operated at NRL. The two types of oscillations have different characteristics. Toward the

Manuscript submitted August 27, 1980.

end of this paper, we shall briefly describe the experimental results in the light of the present theoretical study. The details of these experiments have been reported elsewhere.[2]

We shall first [Sec. II] present a quantitative study of the threshold current above which an absolute instability would be excited as a result of internal feedback processes. The influence of velocity spread and resistive wall loss on the threshold current will also be examined. We next consider oscillations caused by external reflections in Section III, where experimental observations of both types of oscillations are reported. The major results are summarized in the abstract. They are explained in greater detail at the beginning of each section.

II. INTERNAL FEEDBACK MECHANISMS—CONDITION FOR THE ONSET OF ABSOLUTE INSTABILITY

When operated near the "grazing condition," the mildly relativistic electron beam of the gyro-TWA interacts most effectively with the waveguide.[4,5] This "grazing condition" is achieved when the longitudinal velocity of the beam is equal to the group velocity of the forward wave of the waveguide mode. If the beam-wave coupling (determined by the current strength and magnetic field match, etc.) is sufficiently weak, the beam will only couple to the forward waveguide mode. The gyro-TWA would then operate according to what is expected of a convective instability.[3] However, if the coupling is sufficiently strong, the backward wave of the guide mode would be excited. The excitation of these backward waves might then provide an internal feedback mechanism, resulting in an absolute instability which would manifest itself as a natural oscillation of the system. (Under these conditions, care must be exercised to intepret the gain curve of the "amplifier".[6])

The critical current which marks the transition to absolute instability depends sensitively on the magnetic field. It is obtained by using the stability criterion of Briggs and Bers.[3] The analysis is based on the assumption that the system is infinitely long. The characteristic frequency and wavenumber at the transition based on such an analysis would, however, shed light on the required length (starting length) of the system if it is to avoid these natural oscillations.

The result is summarized as follows. If both velocity spread and wall resistivity are absent, and if the applied magnetic field is maintained near the grazing condition, a convective instability sets in at a relatively low current. This convective instability becomes an absolute one if the current (beam strength) exceeds a certain critical value. This critical value is given analytically [cf. Eq. (10)] in terms of the waveguide dimension, electron parallel and perpendicular velocities, and the applied magnetic field. At the onset of the absolute instability, the oscillation frequency and the axial wavenumber are also given analytically. It is found that typically the oscillation frequencies are almost identical (but slightly less than) with the cut-off frequency of the waveguide. We found that velocity spread in the beam has virtually no effect on the threshold current for the transition to absolute instability. The presence of a small amount of distributed wall resistivity would, however, raise the threshold current significantly. It can be shown that such a distributed wall loss does not significantly reduce the gain of the amplifier.[7] In this regard, the presence of wall resistivity offers the best hope to render the amplifier stable at high current level.

In Section II-a, we present the details of the analysis for the case of a cold beam situated in a lossless waveguide. The method developed there has been extended to the studies of a beam with finite temperature in Section II-b. Finally, in Section II-c, we present the results for a lossy waveguide.

a. Cold Beam, Lossless Waveguide:

The typical configuration of a gyro-TWA (Fig. 1) consists of an annular electron beam propagating inside a waveguide of circular cross section of radius r_w. The electrons, guided by a uniform magnetic field ($B_0\, e_z$), move along helical trajectories. Ideally, all electrons have the same perpendicular velocity $v_{\perp 0}$, and the same parallel velocity (v_{z0}), with their guiding centers uniformly distributed on a surface of constant radius r_0 (Fig. 1). The dispersion relation for the interaction between this cold beam and the TE_{mn} waveguide mode (m, n being, respectively, the azimuthal and radial mode numbers) at the s-th cyclotron harmonic frequency has been derived in Ref. (5). It reads

$$\omega^2 - k_z^2c^2 - k_{mn}^2c^2 = \frac{-4\nu c^2}{\gamma_0 r_w^2 K_{mn}} \left[\frac{(\omega^2 - k_z^2c^2)\,\beta_{\perp 0}^2 H_{sm}\,(k_{mn}r_0,\ k_{mn}r_{L0})}{(\omega - k_z v_{z0} - s\Omega_c)^2} - \frac{(\omega - k_z v_{z0})\,Q_{sm}\,(k_{mn}r_0,\ k_{mn}r_{L0})}{\omega - k_z v_{z0} - s\Omega_c} \right], \tag{1}$$

where ω is the frequency of the mode, k_z is the axial wavenumber, $\gamma_0 = (1 - v_{\perp 0}^2/c^2 - v_{z0}^2/c^2)^{-1/2}$, $\beta_{\perp 0} = v_{\perp 0}/c$, $\Omega_c = eB_0/\gamma_0 mc$, $r_{Lo} = v_{\perp 0}/\Omega_c$, $k_{mn} = X_{mn}/r_w$, X_{mn} is the n-th root of $J'_m(x) = 0$, $J_m(x)$ is the Bessel function of order m, $J'_m(x) = dJ_m(x)/dx$, $\nu \equiv Ne^2/mc^2$ is a dimensionless beam density parameter, N is the number of electrons per unit axial length, and the functions K_{mn}, H_{sm}, Q_{sm} are defined as follows:

$$K_{mn} = J_m^2(X_{mn})\,[1 - m^2/X_{mn}^2],$$
$$H_{sm}(x,y) = \left[J_{s-m}(x)J'_s(y)\right]^2,$$

and

$$Q_{sm}(x,y) = 2H_{sm}(x,y) + y \left[J_{s-m}^2(x)J'_s(y)J''_s(y) + \frac{1}{2} J_{s-m-1}^2(x) \cdot J'_s(y)J'_{s-1}(y) - \frac{1}{2} J_{s-m+1}^2(x)J'_s(y)J'_{s+1}(y) \right].$$

Instability occurs at wave frequency and axial wavenumber such that $\omega^2 - k_z^2c^2 - k_{mn}^2c^2 \cong 0$ and $\omega - k_z v_{z0} - s\Omega_c \cong 0$. Hence the second term on the right hand member of Eq. (1) can usually be ignored in comparison with the first term. We can further approximate $\omega^2 - k_z^2c^2$ by $k_{mn}^2c^2$ in the right hand side of (1). Thus, Eq. (1) is simplified to

$$(\omega^2 - k_z^2c^2 - k_{mn}^2c^2)\,(\omega - k_z v_{z0} - s\Omega_c)^2 = -\frac{4\nu c^2}{\gamma_0 r_w^2 K_{mn}} (k_{mn}^2c^2)\,\beta_{\perp 0}^2\,H_{sm}. \tag{2}$$

Henceforth, we shall concentrate on the stability analysis according to Eq. (2).

It is convenient to normalize the frequency ω with respect to the cutoff frequency $\omega_c \equiv k_{mn}c$ and k_z to k_{mn}. Then Eq. (2) is written in dimensionless form as

$$(\bar{\omega}^2 - \bar{k}^2 - 1)(\bar{\omega} - \bar{k}\beta_{\parallel} - b)^2 = -\epsilon, \tag{3}$$

where $\bar{\omega} \equiv \omega/\omega_c$; $\bar{k} \equiv k_z/k_{mn}$; $\beta_{\parallel} \equiv v_{z0}/c$; and the dimensionless parameters b and ϵ are defined by

$$b \equiv s\Omega_c/\omega_c \tag{4a}$$

$$\epsilon \equiv \frac{4\nu c^2\beta_{\perp 0}^2 H_{sm}}{\gamma_0 r_w^2 K_{mn}\omega_c^2}. \tag{4b}$$

Note that b is proportional to the magnetic field and ϵ is a measure of the beam strength. Typically, ϵ is a very small number, on the order of 10^{-5} (or even less). As an example[2], take $m = .0$, $s = n = 1$, $\beta_{\perp 0} = .4$, $\beta_{\parallel 0} = .266$, $\omega_c/2\pi = 34.3$ GHz, $r_w = .533$ cm. Then

$$\epsilon = 3.78 \times 10^{-6} I \tag{4c}$$

where I is the beam current in units of ampere.

In the limit of zero beam strength ($\epsilon = 0$) the waveguide modes

$$\bar{\omega}^2 - \bar{k}^2 - 1 = 0, \tag{5a}$$

and the beam mode

$$\bar{\omega} - \bar{k}\beta_{\parallel} - b = 0, \tag{5b}$$

are decoupled [cf. Fig. (2)]. The coupling of these two modes is strongest when the dispersion curve of the beam mode is tangent to the waveguide mode [cf. Fig. (2)]. This occurs when the magnetic field is adjusted so that $b = b_0$, where

$$b_0 \equiv (1 - \beta_{\parallel}^2)^{1/2}. \tag{6}$$

In the following, we shall assume that $\beta_{\parallel}$ is fixed, and that b is in the vicinity of b_0. We shall then study the properties of the dispersion relation (3) as ϵ, the beam strength, is varied. This way of fixing parameters is suitable for comparison with experiments.[1,2]

We state here the principal results. The details of derivations of these results are given in the Appendices.

(i) If $b \geq b_0$, there is an instability whenever $\epsilon > 0$. This instability can either be convective or absolute. These statements are proven in Appendix A.

(ii) If $b = b_0$ (i.e., exact grazing condition), there is a convective instability if $0 < \epsilon < \epsilon_{cg}$. This instability becomes an absolute one when $\epsilon > \epsilon_{cg}$ where ϵ_{cg} is defined by

$$\epsilon_{cg}^{1/4} = (27)^{1/4} \sqrt{\beta_{\parallel}}\, \bar{k}_{sg}, \tag{7}$$

$$\bar{k}_{sg} = (\bar{\omega}_{sg} - b_0) / 4\beta_{\parallel}, \tag{8}$$

$$\bar{\omega}_{sg} = \frac{(b_0 + 6\sqrt{2}\,\beta_{\parallel}^2)}{1 + 8\beta_{\parallel}^2}. \tag{9}$$

Furthermore, at the onset of the absolute instability, (i.e., $\epsilon = \epsilon_{cg}$), the characteristic wavenumber $\bar{k}_{sg}$ and frequency $\bar{\omega}_{sg}$ are given by Eqs. (8) and (9) respectively. Note that the wavenumber at the onset of absolute instability is purely real. This general result is demonstrated in Appendix B. The proof of the rest of the statements in this paragraph is given in Appendix C.

(iii) For $b \cong b_0$, the onset of the absolute instability occurs when $\epsilon = \epsilon_c$, where ϵ_c is defined by

$$\epsilon_c^{1/4} = (27)^{1/4} \sqrt{\beta_{\parallel}}\, \bar{k}_s, \tag{10}$$

$$\bar{k}_s = \frac{1}{4\beta_{\parallel}} (\bar{\omega}_s - b), \tag{11}$$

$$\bar{\omega}_s = \frac{b + [8\beta_{\parallel}^2(1-b^2) + 64\beta_{\parallel}^4]^{1/2}}{1 + 8\beta_{\parallel}^2} \tag{12}$$

Again, $\bar{k}_s$ and $\bar{\omega}_s$ are respectively the wavenumber and frequency of oscillation at the onset of the absolute instability. It is clear that Eqs. (10)-(12) reduce to (7)-(9) when $b = b_o$, i.e., when the gyro-TWA is operated exactly at the grazing condition.

The numerical values of the critical beam strength, as well as the corresponding frequency of oscillations and wavenumber, can readily be computed for various values of $\beta_{\parallel}$ and b from Eqs. (7)-(12). Listed in Table 1 are the values generated from Eqs. (7)-(9) which physically correspond to the exact grazing condition. Note from the last column of this table that the threshold beam current (measured by ϵ_{sg}) increases with $\beta_{\parallel}$. This result can readily be threshold beam current (measured by ϵ_{sg}) increases with $\beta_{\parallel}$. This result can readily be understood by noting that at higher axial beam velocity, disturbances convect away at a higher rate. To couple the forward propagation of disturbances with the backward waveguide mode, a condition for the excitation of absolute instabilities[3], a stronger current is required. In Table 2, we fix $\beta_{\parallel}$ at .266. We then calculate the threshold current at various values of magnetic field strength. We note that if the magnetic field is below the grazing value, a higher beam current is necessary in order to excite the absolute instability, because the beam mode and the waveguide mode are away from perfect synchronism. If the magnetic field is above the grazing value, the unstable spectrum readily extends to negative values of k_z and the absolute instability is easily excited. In the event that the beam mode (Fig. 2) intersects with the backward waveguide mode

the absolute instability sets in as long as the beam current is non zero. In the last two columns of Table 2, we have assumed that the threshold current I is related to ϵ by Eq. (4c). Note further that the oscillation frequency of these oscillations is slightly less than the cutoff frequency of the waveguide.

In the current gyro-TWA experiments at NRL[1,2], $\beta_{\parallel} = .266$, $\omega_c/2\pi = 34.3$ GHz and $k_{mn} = 7.18\ cm^{-1}$ for the TE_{01} mode. If the magnetic field is maintained at the grazing condition ($b/b_0 = 1$) then an oscillation at a frequency of 34.26 GHz is predicted to occur when the beam current is raised beyond .588 amps as a result of absolute instability [cf., Row (5) in Table II]. Experimentally, an oscillations at 34.27 GHz was indeed observed[8] at a beam current of 1 amp as the magnetic field is raised to the vicinity of the grazing condition. The actual threshold current observed should be somewhat higher than the predicted value as the latter was made for an infinitely long waveguide whereas in reality a finite length waveguide was used and coupling out the ends was not included in the present calculation. We shall discuss in greater detail the experimental results in Section III.

b. Warm Beam, Lossless Waveguide:

We have studied the effects of the velocity spread and energy spread on the threshold current above which an absolute instability is excited. In the NRL gyro-TWA experiments, the energy spread is minimal, of order 1% or less. The spread in the longitudinal velocity is considerably higher, on the order of 10 per cent. We found that, even if the velocity spread is as high as 20 percent, it has a negligible influence on the threshold current. In other words, momentum spread cannot stabilize the absolute instability. This seemingly surprising result can be understood as follows. The presence of an absolute instability requires the backward waveguide mode to be coupled to the forward beam mode[3]. The axial wavenumber k_z is thus constraint to a value in the vicinity of zero at the transition. [See also column 3 of Table II]. Now, the velocity spread $<\Delta v_z>$ modifies the dispersion relation by an amount on the order of $(k_z <\Delta v_z>^2/\omega_c^2$, which is an exceedingly small quantity at the transition to the absolute instability by virtue of small value of k_z, leaving the threshold current calculated in the previous subsection essentially unchanged.

The above conclusions stem from our analysis of the dispersion relation which includes the effect of velocity spread and energy spread, measured respectively by $<\Delta v_z>/v_{z0}$ and $<\Delta\gamma>/\gamma_0$. Assuming that these quantities are small, we obtain the dispersion relationship

$$(\bar{\omega}^2 - \bar{k}^2 - 1)\left[(\bar{\omega} - \bar{k}\beta_{\parallel} - b)^2 - \left[\bar{k}\beta_{\parallel}\frac{<\Delta v_z>}{v_{z0}}\right]^2 - \left[\bar{\omega}\ \frac{<\Delta\gamma>}{\gamma_0}\right]^2\right] = -\epsilon. \tag{13}$$

This equation can readily be compared with Eq. (3), where the symbols are defined. Equation (13) can be deduced from the one obtained by Uhm[9] who applied the idealized "water-bag" electron beam distribution function to the formulation developed earlier.[10]

Applying the techniques developed in the Appendices, we found that a velocity spread less than twenty percent has virtually no effect on the transition current, for reasons explained above. An energy spread less than half a percent actually slightly lowers the threshold current.

It should be emphasized that, while the momentum spread is not effective in suppressing the absolute instability, it can reduce the gain and bandwidth of the amplifier significantly[1]. Once the frequency of the input signal is above the cutoff frequency of the waveguide, k_z will increase significantly (in comparison with a value close to zero). The velocity spread will then have a significant effect on the gain [cf. Eq. (13)]. This observation is corroborated by the numerical studies on the gain and bandwidth of the amplifier reported in Refs. (1) and (7).

c. Cold Beam, Lossy Waveguide:

An attempt to stabilize the gyro-TWA is to coat the inner wall of the metallic waveguide with a layer of material of finite electrical conductivity, such as graphite.[8] A detail study of the effect of a resistive wall on the gain of the gyro-TWA is beyond the scope of this paper. Here we concentrate only on the dependence of threshold current on wall resistivity. It is found that even a small amount of wall loss increases the threshold current substantially.

Let δ be the skin depth of the wall material of the waveguide. Typically, $\delta/r_w << 1$ where r_w is the wall radius. In the limit of small δ/r_w, the dispersion relation reads[7]

$$\left\{\bar{\omega}^2 - \bar{k}^2 - \left[1 - \frac{\delta}{r_w}(i-1)\right]\right\}(\bar{\omega} - \bar{k}\beta_{\parallel} - b)^2 = -\epsilon \tag{14}$$

which is again to be compared with Eq. (3). In obtaining Eq. (14), we have ignored the effect of velocity spread as it can hardly modify the threshold current. In passing, we remark that in the resistive wall experiments to be performed at NRL[8], $\delta/r_w \cong 2.6 \times 10^{-3}$, and that values of δ/r_w as high as 10^{-2} are reasonable in practice.

The analysis of Eq. (14) for the threshold current is more involved and will not be detailed here. Shown in Fig. (3) are the results. To obtain the data in this figure, we fix $\beta_{\parallel} = .266$. The various curves correspond to different magnetic fields. They illustrate the threshold current as a function of δ/r_w (wall resistivity). It is seen that a small amount of wall resistivity can significantly increase the threshold current. That is, wall resistivity may render the gyro-TWA stable against the absolute instability. Shown in Table III are the data for $b/b_o = .98$ at the transition. Again, we have assumed that the beam current I is related to ϵ by Eq. (4c) in obtaining these results.

The increase of threshold current with wall resistivity may be understood qualitatively as follows. As the frequency of oscillation at transition is below the cutoff frequency of the waveguide, the backward wave of the waveguide mode attenuates in the *reverse* direction of beam propagation. This attenuation rate increases as wall resistivity (δ/r_w) increases. For an absolute instability to be excited, this attenuation rate must match the amplification rate of the forward beam mode. This matching requirement is just the alternative statement that a saddle point (i.e., merging of roots of k at a single frequency) must be present for the onset of absolute instability.[3] A higher beam current is thus needed to excite the absolute instability when wall resistivity is present. Note again that the oscillation frequency is just below the cutoff frequency of the waveguide at the transition, and that $\bar{k}_c$ is complex for reasons given above.

We point out that the internal feedback mechanism has recently been theoretically analyzed by Etlicher and Buzzi.[11] However, the main stabilizing influence of wall resistivity has not been included in their calculations. Their work, reported in a conference abstract[11], does not contain sufficient detail for a direct comparison with our work.

III. EXTERNAL FEEDBACK MECHANISMS AND EXPERIMENTAL OBSERVATIONS OF OSCILLATIONS.

Treating the length of the amplifier as infinite we study in the previous section the convective and absolute nature of the cyclotron maser instability. When an absolute instability first sets in, the frequency of oscillations is predicted to be just slightly less than the cutoff frequency of the waveguide. The axial wavenumber is typically 1/30 the transverse wavenumber of the waveguide. Thus, a short interaction length (as well as a resistive wall) may reduce the danger of exciting absolute instabilities.

In reality the gyro-TWA system is finite in length and an additional mechanism for oscillation is provided by partial reflections of the amplifying waves at the ends of the system. At high beam currents, the e-folding length of spatial amplification is very short, and a slight mismatch may convert an amplifier into an oscillator. Based on this argument, one can see that oscillations due to end reflection will inevitably set in at a high current level, regardless of how small a mismatch there is at the ends of the device. Oscillations induced by end reflections, as well as their suppressions, are well-known in the technology of travelling wave tubes. For the present case of the gyro-TWA, this type of oscillations will have frequencies higher than the cut-off frequency of the waveguide for only then would the gain of the amplifier be significant.[1] These statements appear to have been corroborated by the NRL experiments to be decribed below. Again, a resistive wall can (1) render the amplifier stable against this type of oscillations, and at the same time, (2) increase the bandwidth of the amplifier, without significantly sacrificing its gain.[7]

Instabilities have been routinely observed[2,8] during experimental operation of gyro-TWA operating in the TE_{01} circular-electric mode at 35.1 GHz at NRL. The physical design of the gyro-TWA uses a 0.533 cm radius, for a cutoff frequency of 34.30 GHz, copper waveguide 21 cm long. The parameters of the beam were designed to be $v_{\parallel} = .27\ c$ and $v_{\perp} = .40\ c$. Typical linear (small signal) gains obtained were 24 db at a 3 ampere beam current and 32 db at 9 amps.

Typical oscillations occur at several discrete frequencies normally just above cutoff at 34.30 GHz, such as 34.38 GHz and 34.45 GHz. The power output of these oscillations is typically on the order of

the maximum saturated output during stable amplification. These oscillations can be induced from a stably operating amplifier by increasing the beam current and/or the magnetic field hence increasing the gain. These oscillations can be explained as follows.

The gyro-TWA is operated near the cutoff frequency of the interaction waveguide. The mechanism actually has considerable gain almost down to cutoff.[1] Even though the input and output couplers were carefully designed for low reflections throughout the useful bandwidth of the gyro-TWA, matching becomes impossible as the cutoff frequency is approached. Thus, reflection spikes are obtained near cutoff. Cold test reflection measurements indeed reveal reflections at the problem frequencies, namely, at 34.38 GHz and 34.45 GHz.

As the gyro-TWA beam current or magnetic field is increased the gain near cutoff is increased. The reflections constitute a feedback and when the net loop gain exceeds loop losses then oscillation sets in. This is evidenced by the oscillations at 34.38 GHz and at 34.45 GHz reported above.

Instability at just below empty waveguide cutoff has also been observed and is believed to be the absolute instability predicted in Sec. II. The conditions are as follows. At a beam current of 1 amp and cathode voltage of -70 kV, the magnetic field was scanned. The gain measured at 35.13 GHz peaked at 12.7 dB with 1230 watts output (unsaturated) at a magnetic field of 12.81 kG. As the magnetic field was increased the gain (at 35.13 GHz) dropped rapidly to ~0 db at 13.11 kG. Self-oscillation in the TE_{01}^{0} mode at 34.45 GHz set in at a magnetic field of 13.15 kG at a power output level of 8.71 kW. This power level is on the order of maximum observed saturated amplifying power level. An observed (stable) maximum output power at saturation at 1 amp beam current was 5.75 kW with 4.3 db gain. As the magnetic field was raised the oscillations at 34.45 GHz continued. At 13.37 kG the 34.45 GHz oscillation ceased and another oscillation at 34.27 GHz was observed. This oscillation, slightly below the TE_{01}^{0} cutoff, had an output power of 200 watts. At 13.41 kG the power output in this oscillation increased to 660 watts.

The experimental data reported here is limited. At the time the data was taken [1] we were unaware of potential absolute instabilities or their characteristics. Close attention will be made to absolute instabilities in future experiments. However, we tentatively interpret the above data as follows.

As the magnetic field is increased to the peak gain point measured at 35.13 GHz (corresponding to a grazing condition), the gain near cutoff, i.e., 34.30 GHz to 34.50 GHz, is too low to sustain reflection type oscillations. As the magnetic field is increased past the peak gain point (at 35.13 GHz) the gain is still increasing near cutoff until sufficient loop gain is attained for oscillation at 34.45 GHz. As the magnetic field is increased beyond grazing, the threshold current for the absolute instability rapidly decreases. When the absolute instability becomes dominate, then oscillation occurs in that mode. The calculations of the threshold indicate that the absolute instability should occur even at grazing, i.e., the calculated threshold current is 0.588 amp. However, the calculation was made for an infinitely long waveguide when realistically a finite length waveguide was used and coupling out the ends was not included. Thus we would expect the actual threshold to be somewhat higher than indicated in Table II. The lower power level output seems reasonable since the power is essentially coupled out the end rather than propagated out.

We then have several points supporting our belief in the observation of the absolute instability. (i) The oscillation was slightly below cutoff in TE_{01}^{0} mode exactly at the predicted value; (ii) the power output level was substantially lower than the routinely observed reflective oscillations indicating a different type of instability; and (iii) as predicted, the absolute instability set in as the magnetic field was raised. Although the reflection type instability seems to be the most dominant, especially at higher current levels, this absolute instability could be important in gyro-TWA design with regard to methods of overall stabilization.

An attractive method to suppress both types of oscillations is to add loss to the circuit to decrease the loop gain. This also raises the threshold current for the excitation of absolute instabilities. Furthermore, calculations[7] show that the forward gain in a distributed loss waveguide circuit is only decreased by approximately one-third the cold tube loss in dB per unit length. Thus stability would be

obtained with only a slight decrease in forward gain. In addition, wall loss leads to bandwidth improvement.

ACKNOWLEDGMENT

We gratefully acknowledge useful conversations with Drs. M. Baird, A. Drobot, and B. Hui. This work is supported in part by NAVELAX, Task XF 54581 007.

REFERENCES

1. J.L. Seftor, V.L. Granatstein, K.R. Chu, P. Sprangle and M.E. Read, "The Electron Cyclotron Maser as a High-Power Travelling Wave Amplifier of Millimeter Waves," IEEE J. Quantum Electronics Vol. QE-15, pp. 848-853 (1979).

2. L.R. Barnett, K.R. Chu, J.M. Baird, V.L. Granatstein, and A.T. Drobot," Gain, Saturation, and Bandwidth Measurements of the NRL Gyrotron Travelling Wave Amplifier," IEDM Technical Digest, pp. 164-167, (Dec. 1979).

3. R.J. Briggs, *Electron Stream Interaction with Plasma*, MIT Press, Cambridge, Mass. (1964).

4. K.R. Chu, A.T. Drobot, H.H. Szu, and P. Sprangle, "Theory and Simulation of the Gyrotron Travelling Wave Amplifier Operating at Cyclotron Harmonics," IEEE Trans. MTT, Vol. MTT-28, pp. 313-317 (1980).

5. K.R. Chu, A.T. Drobot, V.L. Granatstein and J.L. Seftor, "Characteristics and Optimum Operating Parameters of a Gyrotron Travelling Wave Amplifier," IEEE Trans. Microwave Theory Tech., Vol. MTT-27, pp. 178-187 (1979)

6. See, e.g., Ref. 3, p. 38, 131,167.

7. Y.Y. Lau and K.R. Chu, and L. Barnett, "Effects of Velocity Spread and Wall Resistivity on the Gain and Bandwidth of the Gyrotron Travelling Wave Amplifier," to be published.

8. L. Barnet, et. al., to be published.

9. H.S. Uhm and R.C. Davidson, "Influence of Energy and Axial Momentum Spreads on the Cyclotron Maser Instability in Intense Hollow Electron Beams," Phys. Fluids, Vol. 22, pp. 1804-1810 (1979)

10. K.R. Chu, "Theory of Electron Cyclotron Maser Interaction in a Cavity at the Harmonic Frequencies," Phys. Fluids, Vol. 21, pp. 2354-2364 (1978).

11. B. Etlicher and J.M. Buzzi, "Study of the Synchrotron Maser Absolute Instabilities", Third International Topical Conference on High Power Electron and Ion Beam Research and Technology (July 3-6, 1979, Novosibirsk, USSR, p. 105).

12. A.W. Trielpiece and R.W. Gould, "Space Charge Waves in Cylindrical Plasma Columns," J. Applied Phys. Vol. 30, pp. 1784-1793 (1959).

APPENDIX A

Presence of an Instability Whenever $b \geqslant b_0$.

In this Appendix, we prove that there is always an instability (which can either be absolute or convective) whenever the magnetic field is higher than that at the grazing condition. It suffices[3] to show that, whenever $\epsilon > 0$ and $b \geqslant b_0$, there is always a pair of complex roots of $\bar{\omega}$ for some real values of $\bar{k}$, say, at $\bar{k} = \beta_{11}/b$. With $\bar{k} = \beta_{11}/b$, Eq. (3) can be written as

$$(y^2 - 1)(y - a)^2 = -\epsilon_1, \tag{A1}$$

where

$$y \equiv \bar{\omega} b/(b^2 + \beta_{11}^2)^{1/2}, \tag{A2}$$

$$a \equiv (\beta_{11}^2 + b^2)^{1/2}, \tag{A3}$$

$$\epsilon_1 \equiv \epsilon\, b^4/(b^2 + \beta_{11}^2)^2. \tag{A4}$$

Note that

$$a \geqslant 1 \tag{A5}$$

since

$$\beta_{11}^2 + b^2 = 1 + (b^2 - b_0^2) \geqslant 1 \quad \text{if} \quad b \geqslant b_0.$$

As a function of y, $f(y) \equiv (y^2 - 1)(y - a)^2$ is sketched in Fig. 4. As easily seen from this figure, the equation $f(y) = -\epsilon_1$ admits at least a pair of complex roots of y whenever $\epsilon_1 > 0$. From (A2) and (A4), we conclude that $\bar{\omega}$ has at least a pair of complex roots as long as $\epsilon > 0$.

APPENDIX B

Onset of Absolute Instability at Real Values of k.

In this Appendix, we prove that when an absolute instability first sets in, the wavenumber is always real. This result is useful because it considerably restricts our search in wavenumber space in the calculation of the critical beam strength that marks the transition to absolute instability.

At the transition, the frequency $\bar{\omega} = \bar{\omega}_s$ is real. For this value of $\bar{\omega}_s$, there is a double root[3] of $\bar{k}$. Below, we prove that this double root is real.

Since $\bar{\omega} = \bar{\omega}_s$ is real, and Eq. (3) is a fourth degree polynomial of $\bar{k}$ with *real* coefficients, all four roots $\bar{k}_1$, $\bar{k}_2$, $\bar{k}_3$, $\bar{k}_4$ of Eq. (3) must either be real or appear as complex conjugate pairs. We shall first assume that the above-mentioned double root has a nonvanishing imaginary part and then show that a contradiction results.

Denote the real and imaginary part of the double root $\bar{k}_1$, $\bar{k}_2$ to be k_{sr} and k_{si}. If $k_{si} \neq 0$, the other two roots $\bar{k}_3$, $\bar{k}_4$ must also be a double root since the roots occur in conjugate pairs. In this case, Eq. (3) may be written as

$$\begin{aligned}
&(\bar{k} - \bar{k}_1)(\bar{k} - \bar{k}_2)(\bar{k} - \bar{k}_3)(\bar{k} - \bar{k}_4) \\
&= (\bar{k} - k_{sr} - i\,k_{si})^2(\bar{k} - k_{sr} + i\,k_{si})^2 \\
&= \bar{k}^4 + \bar{k}^3\,(-4k_{sr}) + \bar{k}^2(6\,k_{sr}^2 + 2\,k_{si}^2) \\
&\quad + \bar{k}\,[-4k_{sr}(k_{sr}^2 + k_{si}^2)] + (k_{sr}^2 + k_{si}^2)^2 = 0.
\end{aligned} \tag{B1}$$

On the other hand, equation (3) may also be written as

$$\begin{aligned}
&\bar{k}^4 + \bar{k}^3\left[2\left(\frac{b - \bar{\omega}_s}{\beta_{\parallel}}\right)\right] + \bar{k}^2\left[\left(\frac{b - \bar{\omega}_s}{\beta_{\parallel}}\right)^2 - (\bar{\omega}_s^2 - 1)\right] \\
&+ \bar{k}\left[-2\,(\bar{\omega}_s^2 - 1)\left(\frac{b - \bar{\omega}_s}{\beta_{\parallel}}\right)\right] - \frac{\epsilon}{\beta_{\parallel}} - (\bar{\omega}_s^2 - 1)\left(\frac{b - \bar{\omega}_s}{\beta_{\parallel}}\right)^2 = 0.
\end{aligned} \tag{B2}$$

Since (B1) and (B2) are the same equation, the coefficients must be the same. Thus,

$$-4k_{sr} = 2(b - \bar{\omega}_s)/\beta_{\parallel}, \tag{B3}$$

$$6k_{sr}^2 + 2k_{si}^2 = \left(\frac{b - \bar{\omega}_s}{\beta_{\parallel}}\right)^2 - (\bar{\omega}_s^2 - 1), \tag{B4}$$

$$-4k_{sr}(k_{sr}^2 + k_{si}^2) = -2(\bar{\omega}_s^2 - 1)\left(\frac{b - \bar{\omega}_s}{\beta_{\parallel}}\right). \tag{B5}$$

Dividing (B3) by (B5), we obtain

$$-(\bar{\omega}_s^2 - 1) = k_{sr}^2 + k_{si}^2. \tag{B6}$$

Using (B6) and (B3), we express the right hand member of (B4) as

$$\left(\frac{b - \bar{\omega}_s}{\beta_{\parallel}}\right)^2 - (\bar{\omega}_s^2 - 1) = 5k_{sr}^2 + k_{si}^2. \tag{B7}$$

Clearly, (B7) contradicts (B4) if $k_{si} \neq 0$. We conclude then that the assumption that $k_{si} \neq 0$ is false. Hence at the transition to absolute instability, the wavenumber $\bar{k}_s$ must be real.

APPENDIX C

Detailed Study of Absolute and Convective Instability at the Grazing Condition.

We shall focus our attention to the case where $b = b_0$. The dispersion relation (3) reads

$$D(\omega,k) \equiv [k^2 - (\omega^2 - 1)]\left[k - \frac{\omega - b_0}{\beta_{||}}\right]^2 = \frac{\epsilon}{\beta_{||}^2}, \tag{C1}$$

where, in this Appendix, we have dropped the bar in ω and k for convenience. Since the beam strength ϵ enters only in the RHS of (C1), we shall examine the detailed property of $D(\omega,k)$. In the present study of transition to absolute instability, we need only to consider real values of ω and k. [Cf. Fig. 5]. Since the onset of an absolute instability always occurs at a multiple root of *real* k (Cf. Appendix B), we need only to focus our attention at those values of k in Figs. 5 for which $D(\omega,k)$ is stationary. Moreover, since $\epsilon \geqslant 0$, only non-negative values of $D(\omega,k)$ are considered.

We first determine the trajectories of the roots in the complex k plane as the imaginary part of ω changes from 0 to $-\infty$. [Cf. Fig. 6a.]* This consideration is necessary to distinguish an absolute from convective instability.[3] As $\omega \rightarrow -i\ \infty$, among the four roots of k in Eq. (C1), three roots would tend to $-i\infty$ and *only* the fourth root would tend to $+i\infty$. Note that the fourth root (let us designate it to be k_4) corresponds to the waveguide mode which propagates in the opposite direction of the beam velocity. If the movement of the roots is in accordance with that depicted in Fig. (6b), a convective instability sets in when ϵ is slightly increased. On the other hand, if the roots move according to Fig. (6c), an absolute instability would set in when ϵ is raised to a higher level. In other words, an absolute instability sets in only if the merging of roots in the k plane involves the backward wave mode of the waveguide. This result perhaps is anticipated from the outset because the internal feedback, which is required for an oscillation, can be provided for only by the wave supported by the waveguide which propagates in the reverse direction of the beam. This wave can be excited only if the beam strength is so high that all modes are strongly coupled.

*We assume that the solutions assume a dependence of $\exp i(\omega t - ikz)$.

From these considerations, we then see that the merging of k roots at $k = \beta_{\parallel}/b_o$ in Fig. (5b) must correspond to the outset of a convective instability since the merging roots arise from the beam mode and the *forward* wave mode of the waveguide. This convective instability sets in as long as $\epsilon > 0$, in agreement with the conclusion of Appendix A. As ϵ is raised slightly above zero, we encounter another double root of k [cf. k_A in Fig. (5c,d)]. This double root of k, however, does *not* correspond to an absolute instability since the merging of the roots does not involve the backward wave of the waveguide mode either.

Examination of Fig. 5 shows that the only multiple root which involves both the backward wave and the (forward) beam mode is k_{sg} as shown in Fig. (5f). Thus the onset of absolute instability occurs when $\epsilon = \epsilon_{cg}$, where ϵ_{cg} is given by [cf. (C1)]

$$\epsilon_{cg} = \beta_{\parallel}^2 D(\omega_{sg}, k_{sg}) \tag{C2}$$

and ω_{sg}, k_{sg} are the *real* root determined from the conditions

$$\left.\frac{\partial D}{\partial k}\right|_{\omega_s, k_s} = 0, \tag{C3}$$

$$\left.\frac{\partial^2 D}{\partial^2 k}\right|_{\omega_s, k_s} = 0. \tag{C4}$$

A little algebra yields the relevant solution

$$\omega_{sg} = \frac{b_0 + 6\sqrt{2}\beta_{\parallel}^2}{1 + 8\beta_{\parallel}^2}, \tag{C5}$$

$$k_{sg} = \frac{1}{4\beta_{\parallel}}(\omega_{sg} - b_0). \tag{C6}$$

These equations are just in Eqs. (9), (8) of the main text. Substitution of (C5) and (C6) into (C2) gives Eq. (7).

A few remarks concerning our calculations are in order. It can readily be shown from Eq. (9) that $\bar{\omega}_{sg}$ is always less than unity. This fact that oscillation may occur at a frequency lower than the cutoff frequency of the waveguide is hardly a surprising result. It is well-known[12] that when a waveguide is loaded with a plasma, modes with a frequency below the cutoff frequency of the waveguide can exist.

In the present case, the waveguide is partially loaded with the beam, which itself constitutes an active medium. This brings out another point which at first sight may also seem a bit paradoxical. At the grazing condition, one may then ask, how can an absolute instability ever exist as the beam mode and the waveguide mode both propagate in the forward direction? The answer is that at very low beam current, both modes are weakly coupled and indeed no absolute instability exists according to the usual notion of coupling of modes. However, as a sufficiently high current level, both modes are strongly coupled. In fact, *all* modes are coupled, including the waveguide mode which propagates in the opposite direction of the beam. The excitation of the latter modes provides an internal feedback and is the basic reason for the possible excitation of an absolute instability. [Cf. Fig. (5f)].

Table I. The dimensionless frequency ($\bar{\omega}_{sg}$) and wavenumber ($\bar{k}_{sg}$) at the onset of absolute instability ($\epsilon = \epsilon_{sg}$) for various $\beta_{\parallel}$. Magnetic field is maintained at the grazing condition.

$\beta_{\parallel}$	b_0	$\bar{\omega}_{sg}$	$\bar{k}_{sg}$	$\epsilon_{sg}^{1/4}$
0	1	1	0	0
.1	0.995	0.99985	0.01216	0.00877
.2	0.9798	0.9994	0.0245	0.0250
.3	0.9539	0.9986	0.0372	0.0465
.4	0.9165	0.9974	0.0506	0.0729
.5	0.8660	0.9958	0.0649	0.1046
.6	0.8000	0.9935	0.0806	0.1423
.7	0.7141	0.9902	0.0986	0.1881
.8	0.6000	0.9854	0.1204	0.2455
.9	0.4359	0.9771	0.1503	0.3251

Table II. Data for the transition to absolute instability at various magnetic field strength (b/b_0) with $\beta_{\parallel}$ fixed at 0.266. Shown are the normalized characteristic frequency ($\bar{\omega}_s$), wavenumber ($\bar{k}_s$), threshold current (I) and the axial wavelength (λ_z) at the transition.

b/b_0	$\bar{\omega}_s$	$\bar{k}_s$	I (amps)	λ_z (cm)
.92	.990471	.097383	45.42	8.98
.94	.99327	.081894	22.71	10.68
.96	.995634	.065996	9.58	13.25
.98	.997531	.049659	3.07	17.613
1.00	.998920	.032845	0.588	26.625
1.02	.999759	.015514	0.02925	56.377

Table III. Data for transition to absolute instability at various values of wall resistivity (δ/r_w). Here $\beta_{\parallel} = .266$, $b/b_0 = .98$. Note that if $\delta \neq 0$, $\bar{k}_s$ is complex, and that $\bar{\omega}_s \lesssim 1$.

δ/r_w	$\bar{\omega}_s$	$\bar{k}_s$	I (amps)
0	.997531	(.049659, 0)	3.07
.002617	.996291	(.036153, - .05302)	5.567
.005234	.996123	(.02889, - .067291)	7.684
.007851	.996193	(.023109, - .07763)	9.955
.010468	.996391	(.018168, - .08602)	12.391

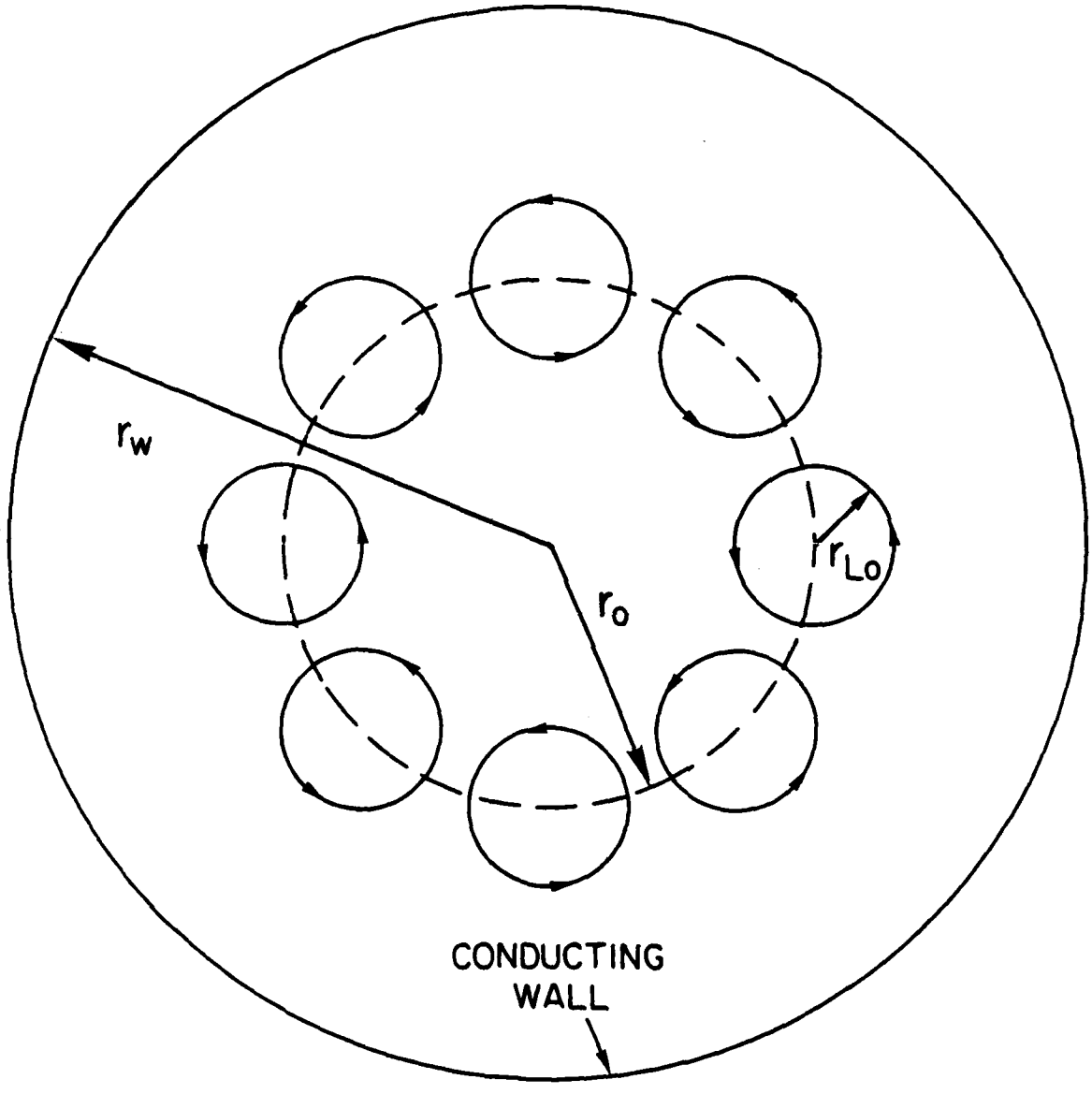

Fig. 1 — Cross sectional view of the gyro-TWA. The applied magnetic field points out of the paper.

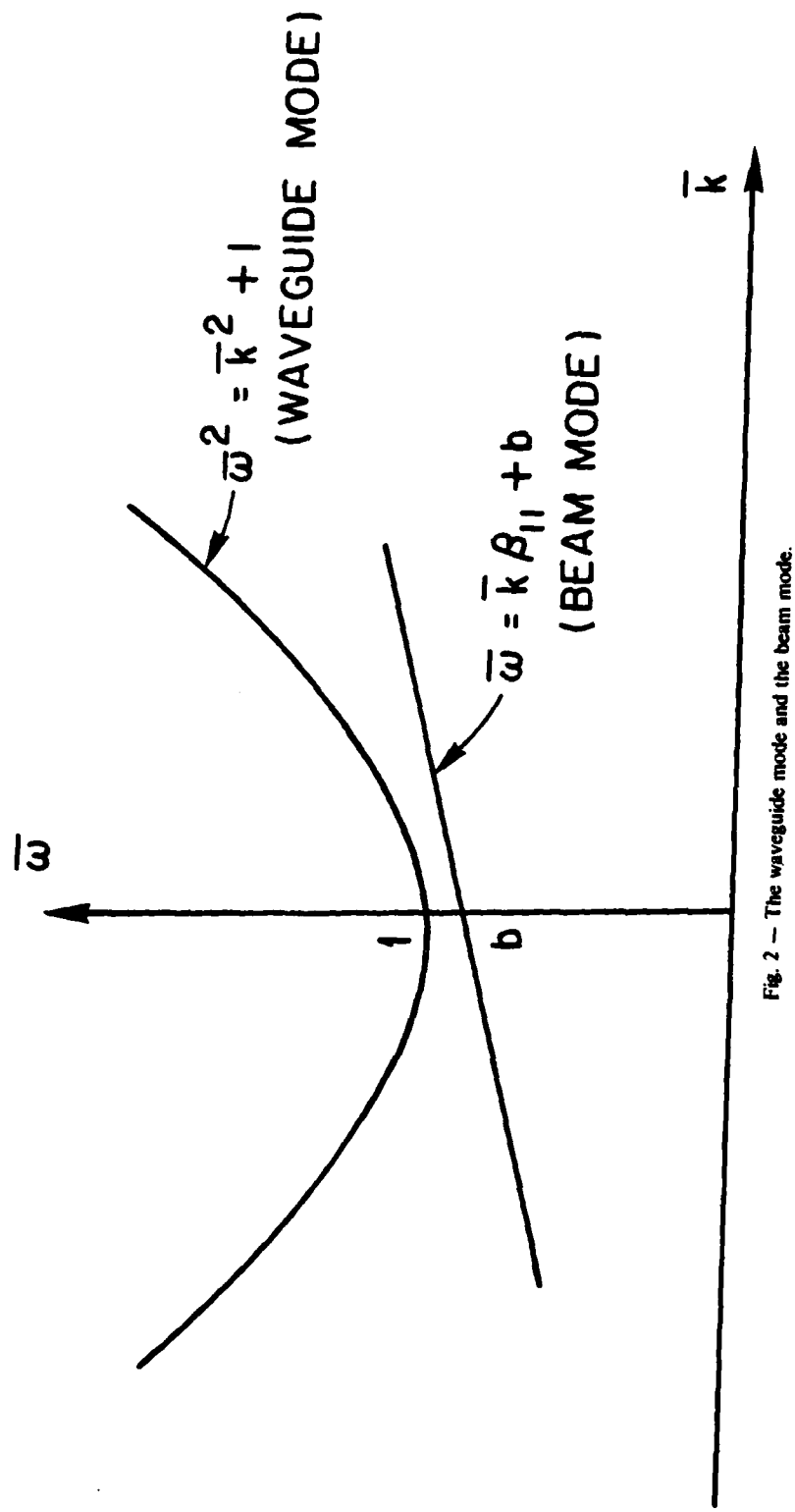

Fig. 2 — The waveguide mode and the beam mode.

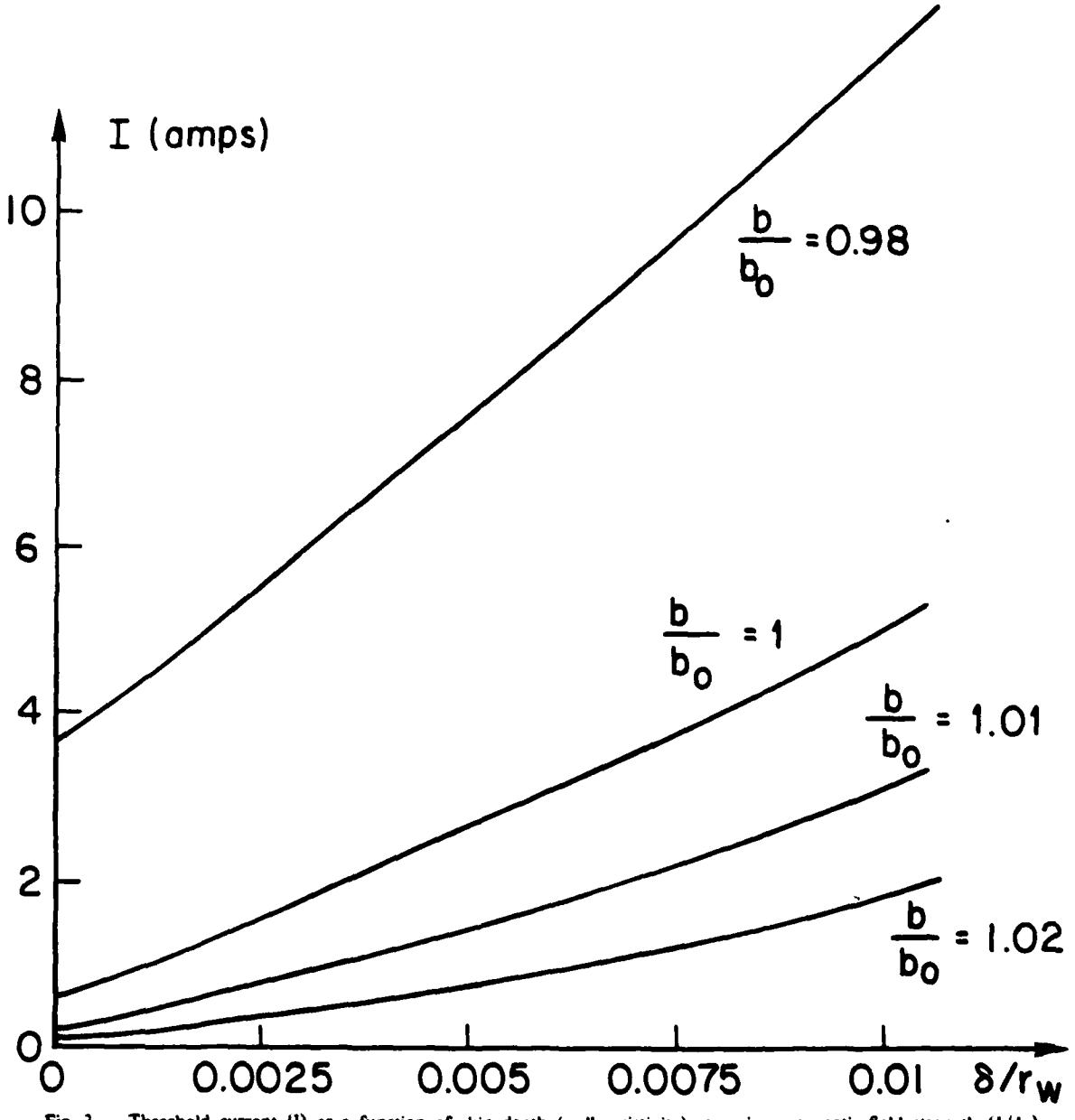

Fig. 3 — Threshold current (I) as a function of skin depth (wall resistivity) at various magnetic field strength (b/b_0). Here $\beta_{11} = 0.266$, $\omega_c/2\pi = 34.3GHz$ and $r_w = 0.533$ cm.

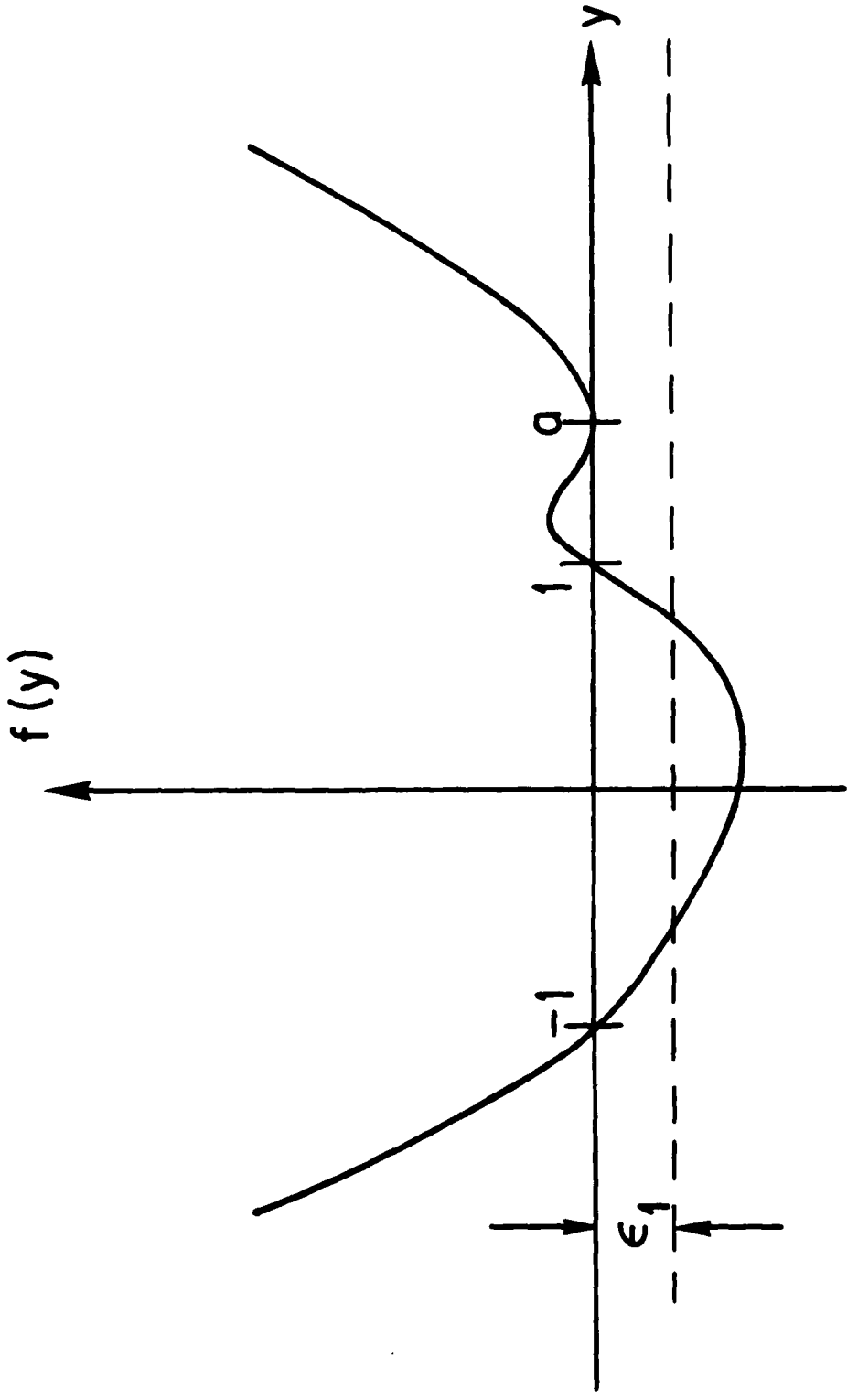

Fig. 4 — Sketch of the function $f(y) = (y^2 - 1)(y - a)^2$

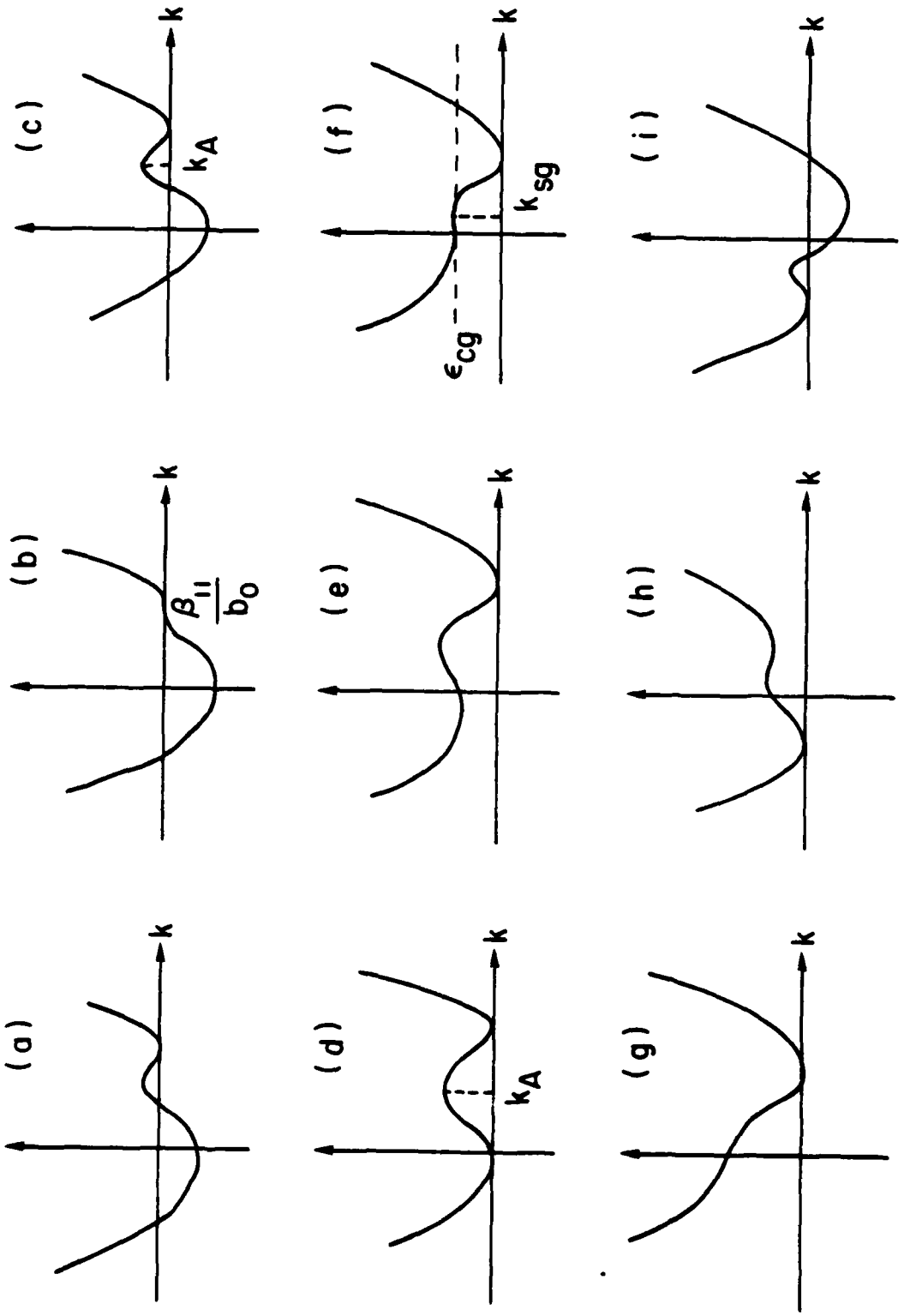

Fig. 5 — Sketches of $\beta_{11}^2 D(\omega,k)$ at various values of ω: (a) $\omega > \frac{1}{b_0}$, (b) $\omega = \frac{1}{b_0}$, (c) $1 < \omega < \frac{1}{b_0}$ (d) $\omega = 1$ (e) $\omega_{sc} < \omega < 1$, (f) $\omega = \omega_{sg}$; (g) $\omega' < \omega < \omega_{sg}$ (h) $-1 < \omega < \omega'$, (i) $\omega < -1$. Here, ω_{sc} and k_{sg} are defined in Eqs. (C5) and (C6) and $\omega' = (b_0 - 6\sqrt{2}\beta_{11}^2)/(1 + 8\beta_{11}^2)$.

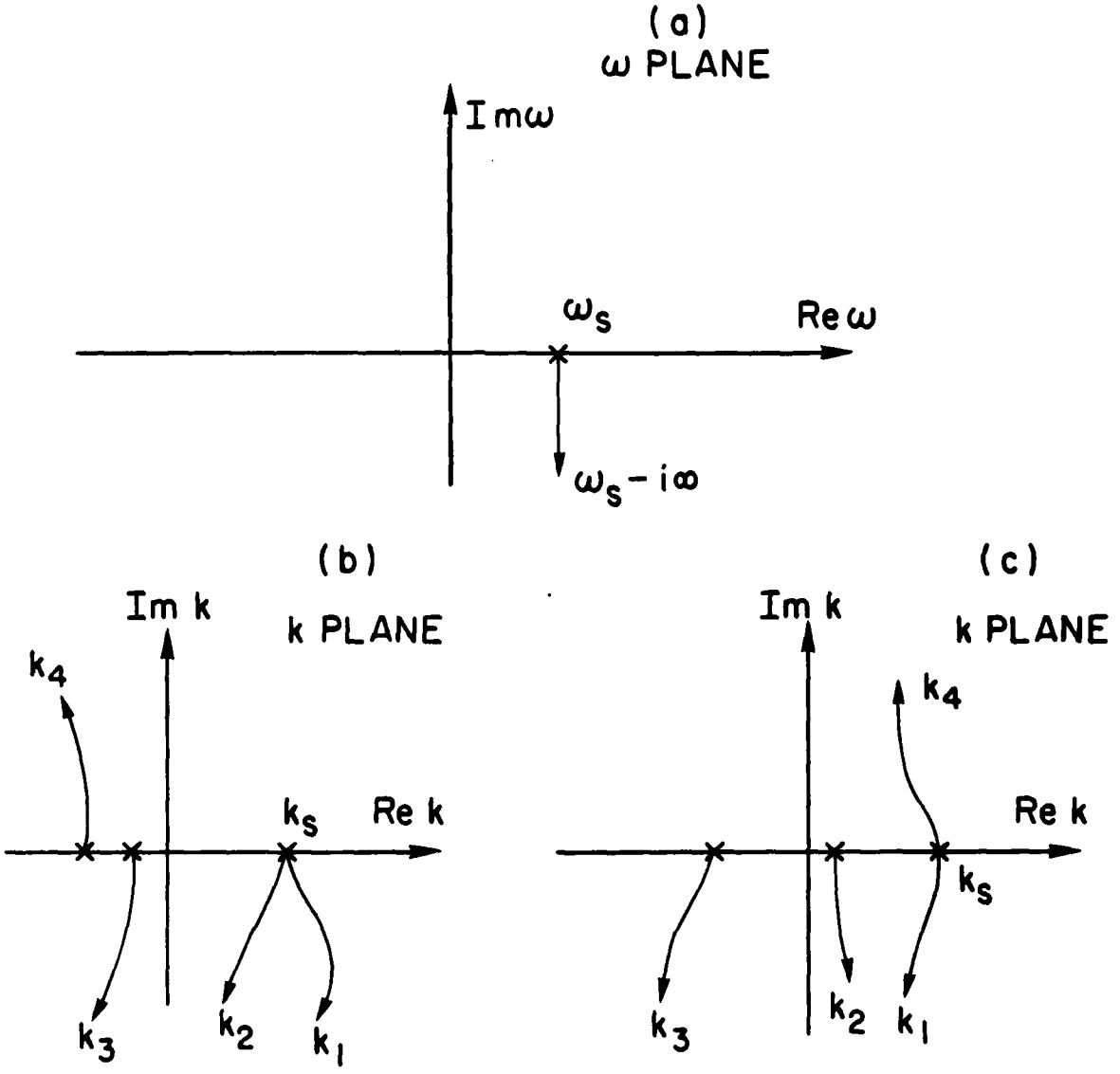

Fig. 6 — Trajectories of the roots in the k plane as ω changes from ω_s to $\omega_s - i\infty$. In (b), a convective instability exists. In (c) k_s corresponds to the onset of an absolute instability.

GYROTRON & ECH DISTRIBUTION LIST

No. of Copies			Addressee
(25) (26)	Naval Research Laboratory Attn: Name/Code 4555 Overlook Avenue, S.W. Washington, D.C. 20375	Code:	4700 - Dr. T. Coffey 4740 - Dr. V.L. Granatstein 4740 - Dr. R.K. Parker 4740 - Dr. K.R. Chu 4740 - Dr. M.E. Read 4740 - Dr. C.W. Roberson 4740 - Dr. S. Gold 4790 - Dr. P.A. Sprangle 4790 - Dr. B. Hui 4790 - Dr. W.M. Manheimer 6850 - Dr. L.R. Whicker 6853 - Dr. A. Ganguly 6805 - Dr. S.Y. Ahn 6805 - N.R. Vanderplaats 6875 - Dr. R. Wagner
	On-Site Contractors:	Code:	4740 - Dr. J.M. Baird (B-K Dynamics) 4740 - Dr. L. Barnett (B-K Dynamics) 4740 - Dr. D. Dialetis (SAI) 4740 - A.J. Dudas (JAYCOR) 4740 - Dr. R.M. Gilgenbach (JAYCOR) 4740 - Dr. K.J. Kim (JAYCOR) 4740 - Dr. Y.Y. Lau (SAI) 4740 - Dr. J.S. Silverstein (HDL) 4790 - Dr. A.J. Drobot SAI) 4790 - Dr. C.M. Hui (JAYCOR) 4790 - Dr. J. Vomvoridis (JAYCOR) 5704S - Dr. S. Smith (LOCUS, Inc.)
(3)	Secretary Department of Energy Attn: Washington, D.C. 20545		Dr. P. Stone (G-234) Dr. M. Murphy (G-234) Dr. J. Willis (G-234)
(1)	Air Force Avionics Laboratory Attn: W. Friz Wright/Patterson AFB, Ohio 45433		
(1)	Bell Laboratories Attn: Dr. W.M. Walsh, Jr. 600 Mountain Avenue Murray Hill, New Jersey 07971		

No. of Copies		Addressee
(1)	Columbia University Department of Electrical Engineering Attn: Dr. S.P. Schlesinger New York, New York 10027	
(1)	Dartmouth College Physics Department Attn: Dr. John Walsh Dartmouth, New Hampshire 03755	
(12)	Defense Technical Information Center Cameron Station 5010 Duke Street Alexandria, Virginia 22314	
(1)	Georgia Institute of Technology Engineering Experimental Station Attn: Dr. James J. Gallagher Atlanta, Georgia 30332	
(3)	Hughes Aircraft Co. Attn: Electron Dynamics Division 3100 Lomita Boulevard Torrance, California 90509	Dr. J.J. Tancredi K. Arnold K. Amboss
(1)	Los Alamos Scientific Laboratory Attn: Dr. Paul Tallerico P.O. Box 1663 Los Alamos, New Mexico 87545	
(1)	Massachusetts Institute of Technology Research Laboratory of Electronics Attn: Dr. G. Bekefi Bldg. 36, Rm. 36-225 Cambridge, Massachusetts 02139	
(3)	Massachusetts Institute of Technology Plasma Fusion Center Attn: 167 Albany St., N.W. 16-200 Cambridge, Massachusetts 02139	Dr. R. Davidson Dr. M. Porkolab Dr. R. Temkin
(1)	Northrop Corporation Defense System Department Electronics Division Attn: G. Doehler 175 W. Oakton St. Des Plaines, Illinois 60018	
(2)	Oak Ridge National Laboratories Attn: P.O. Box Y Oak Ridge, Tennessee 37830	Dr. A. England M. Loring

No. of Copies		Addressee
(1)	Princeton University Plasma Physics Laboratory Attn: Dr. H. Hsuan Princeton, New Jersey 08540	
(2)	Raytheon Company Microwave Power Tube Division Attn: Willow St. Waltham, Massachusetts 02154	R. Edwards R. Handy
(1)	Science Applications, Inc. Attn: Dr. Alvin Trivelpiece 1200 Prospect St. La Jolla, California 92037	
(1)	Stanford University SLAC Attn: Dr. Jean Lebacqz Stanford, California 94305	
(1)	University of Arizona Optical Sciences Center Attn: Dr. W.E. Lamb Tucson, Arizona 85720	
(1)	Varian Associates Bldg. 1 Attn: Dr. H. Jory 611 Hansen Way Palo Alto, California 94303	
(1)	Yale University Mason Laboratory Attn: Dr. J.L. Hirshfield 400 Temple Street New Haven, Connecticut 06520	
(1)	Kings College University of London Attn: Dr. P. Lindsay London, United Kingdom	
(1)	Nagoya University Institute of Plasma Physics Attn: Dr. H. Ikegami Nagoya, Japan 464	
(1)	National Taiwan University Department of Physics Attn: Dr. Yuin-Chi Hsu Taipei, Taiwan, China	

No. of Copies	Addressee
(1)	TFR Group DPH - PFC Attn: Dr. A. Cavallo 92260 Fontenay-auix Roses France
(1)	Thompson C.S.F./DET/TDH Attn: Dr. G. Mourier 2 Rue Latecoere 78140 Velizy Villa conblay France
(1)	UKAEA Culham Laboratory Attn: Dr. A.C. Riviere Abingdon Oxfordshire United Kingdom